PHILOSOPHICAL TRANSACTIONS OF THE ROYAL SOCIETY A MATHEMATICAL, PHYSICAL & ENGINEERING SCIENCES

Influence of Deep-Sea Benthic Processes on Atmospheric CO $_{2}$

E. T. Sundquist

Phil. Trans. R. Soc. Lond. A 1990 **331**, 155-165
doi: 10.1098/rsta.1990.0062

Phil. Trans. R. Soc. Lond. A **331**, 155–165 (1990) [155]
Printed in Great Britain

Influence of deep-sea benthic processes on atmospheric CO_2

By E. T. Sundquist
U.S. Geological Survey, Quissett Campus, Woods Hole, Massachusetts 02543, *U.S.A.*

Understanding ocean–atmosphere carbon-cycle interactions requires attention to the potential importance of marine benthic processes, particularly deep-sea carbonate dissolution. However, because of the wide array of processes that control marine carbonate dissolution rates, it is difficult to identify which processes dominate rates of response to global carbon-cycle perturbations. This paper describes a model that simulates atmospheric CO_2, ocean chemistry and sediment carbonate content in a time-dependent fashion. Response times are assessed through an analysis of a series of perturbation experiments in which a pulse of CO_2 is added to the model atmosphere. The results of these experiments suggest that the relatively rapid buffering of atmospheric CO_2 by seawater is controlled by the rate of ocean mixing and accounts for about 60% of the total buffering by the ocean–sediment system. The more gradual buffering of atmospheric CO_2 and seawater by carbonate sediments is controlled by the rate of sedimentation of carbonate particles, but the rate of this buffering is slower than previously thought because the dissolution or precipitation of carbonates does not produce dissolved carbonate ions on a mole-for-mole basis.

Introduction

The CO_2 content of the atmosphere is very sensitive to global carbon-cycle perturbations, ranging from modern fossil-fuel consumption to glacial–interglacial fluctuations in terrestrial vegetation and ocean circulation. Because of its important influence on both carbon cycling and the radiative balance of the Earth's atmosphere, CO_2 is a critical factor in the complex system of dynamic feedbacks controlling carbon and heat fluxes everywhere on the Earth's surface. It is not surprising, therefore, that even the seemingly remote deep-sea floor is part of the web of global interactions linking atmospheric CO_2 to the global carbon cycle and climate system.

This study focuses in particular on deep-sea dissolution of carbonate sediments as one of the most important processes regulating the response of atmospheric CO_2 to global carbon-cycle and climate perturbations. The dissolution of marine carbonate sediments is very important as a long-term buffering mechanism for anthropogenic CO_2. The sediment record of carbonate dissolution correlates strongly with glacial–interglacial climate fluctuations (Arrhenius 1952) and (at least for the last 160000 years) with variations in atmospheric CO_2 (Barnola *et al.* 1987). Therefore an understanding of sea-floor carbonate dissolution is essential to relating past geologic carbon-cycle and climate changes to present and future anthropogenic perturbations.

One of the most important and poorly understood aspects of marine carbonate dissolution is the rate of its response to any given change. This problem is complicated by the broad range of processes that contribute to the dynamic balance between marine carbonate dissolution and sedimentation rates. It is difficult to identify those processes that dominate rates of response to

global carbon-cycle perturbations. Some processes (such as vertical ocean exchange at relatively shallow depths) can be characterized by timescales of decades, although others (such as the dissolved calcium river flux) can only influence the oceans over timescales of about 100000 years or more. It is clear that other processes are associated with a range of timescales between these extremes. It is very important to clearly define the relative importances of the many processes controlling carbonate dissolution over a broad spectrum of timescales. This effort is essential to fully utilizing the sediment record of past changes to help anticipate the role of carbonate dissolution in the anthropogenic CO_2 perturbation.

This paper describes an attempt to model the atmosphere, oceans and sediments in a manner that encompasses some of the processes and timescales that are most important in characterizing marine carbonate dissolution. The model simulates atmospheric CO_2, ocean chemistry and sediment carbonate content in a time-dependent fashion. Response times are assessed through analysis of a series of perturbation experiments in which a pulse of CO_2 is added to the model atmosphere. Although the analysis is limited by many oversimplifications and uncertainties, it is a first step toward establishing the factors that are most important in determining the rates of carbonate dissolution response to global carbon-cycle perturbations.

Model description

The model used in this study is diagrammed in figure 1. It is a crude approximation of the processes that control interactions among atmospheric CO_2, ocean chemistry and marine carbonate sediments. A more complete description of many aspects of the model can be found in Sundquist (1990). The global oceans are approximated as three regions representing waters south of latitude 50° S, north of latitude 50° N (55° N in the Pacific Ocean) and all waters between these polar regions. Each polar region is represented by two boxes divided vertically at 300 m. The temperate–tropical region is represented by ten boxes separated by boundaries at 100, 300, 500, 700, 1000, 2000, 3000, 4000 and 5000 m. Volumes and areas are calculated using the hypsometric data of Menard & Smith (1986) and Gorshkov (1980).

For each ocean box the speciation of dissolved inorganic carbon is calculated from total alkalinity and total dissolved inorganic carbon for the appropriate temperature, salinity and pressure using empirical equilibrium relationships (Lyman 1957; Culberson & Pytkowicz 1968; Mehrbach *et al.* 1973; Millero 1979; Dickson & Riley 1979) and specific ion ratios (Culkin 1965). Air–sea exchange is calculated using CO_2 solubilities (Weiss 1974) and a gas-exchange coefficient of 7×10^4 mol m^{-2} atm^{-1} a^{-1}† (Broecker *et al.* 1980; Seigenthaler 1983). Ocean mixing is represented by both diffusive and advective terms. Values for eddy diffusivity range from 1.7 cm^2 s^{-1} at the boundary below the temperate ocean surface mixed layer (Li *et al.* 1984) to 0.6 cm^2 s^{-1} in the deep ocean (Ku *et al.* 1980). Following Gordon & Taylor (1975), the formation of Antarctic bottom water is represented by advective flux terms totaling 40×10^6 m^3 s^{-1} from the deep south polar box to the temperate boxes deeper than 3000 m; the formation of North Atlantic deep water is represented by flux terms totaling 10×10^6 m^3 s^{-1} from the deep north polar box to the temperate boxes deeper than 1000 m; and the formation of Antarctic intermediate water is represented by flux terms totaling 20×10^6 m^3 s^{-1} from the south polar surface box to the temperate boxes between 300 and 2000 m. The Antarctic bottom water flux is partially balanced by a deep return advective flux of 20×10^6 m^3 s^{-1} to the deep

† 1 atm ≈ 10^5 Pa.

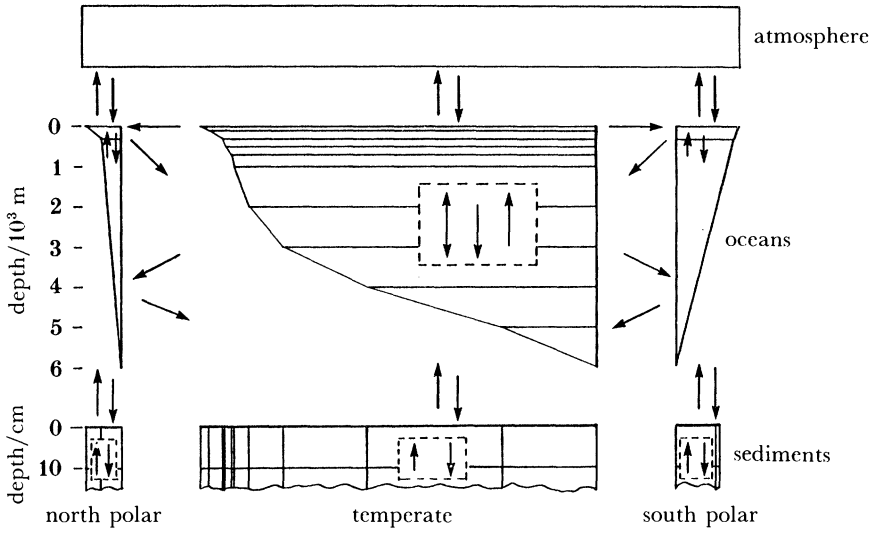

FIGURE 1. The atmosphere–ocean–sediment box model used in this study. The indicated ocean geometry approximates the hypsometric curve used to construct ocean areas and volumes. Arrows indicate generalized exchange fluxes (the double arrow represents ocean diffusive mixing).

south polar box from the temperate box representing waters between 2000 and 3000 m. These flux terms imply additional advective terms representing upwelling throughout the temperate water column.

Each ocean box in the model is coupled to a sediment box represented as a homogeneously bioturbated layer 10 cm thick. The area of the sea–sediment interface for each box is determined by the hypsometric data cited above. Fluxes of calcite and non-carbonate particles are represented as sedimentation terms at the sea–sediment interface. Additional terms for calcite dissolution imply values for the terms for the net sediment flux through the bottom of the bioturbated layer (i.e. the sediment burial flux). The mean calcite fraction of each sediment box is treated as a time-dependent variable derived from the mass balance of the fluxes to and from the bioturbated layer.

The calculation of calcite dissolution fluxes is based on approximations of the sediment calcite content, the depth of the calcite saturation horizon, the carbonate-ion concentrations in bottom waters, and the rates of calcite dissolution in sediment pore waters. The depth of the saturation horizon is determined from the water column carbonate-ion concentrations and saturation carbonate-ion concentrations by interpolation between adjacent ocean boxes. Saturation carbonate-ion concentrations are calculated from the apparent solubilities and partial molal volumes of Ingle (1975). The pore-water dissolution model of Keir (1983) is used to calculate dissolution fluxes. Model experiments were done to assess the importance of the wide range of dissolution rate constants obtained in previous applications of this pore-water model to experiments using calcite suspensions or calcite-rich sediment substrates (Keir 1983).

The ocean–atmosphere–sediment model integrates calcite dissolution fluxes over the sea-floor area exposed to undersaturated conditions. This approach requires the model to independently resolve the time-dependent calcite contents of sediments that are dissolving and those that are not dissolving within any box that is found to contain a saturation horizon. Another model requirement is that it 'remember' the properties of previously buried

sediments, as these sediments may become incorporated into the bioturbated layer if a perturbed dissolution flux exceeds the total sedimentation flux (Sundquist *et al.* 1977).

A reasonable model steady-state solution is a prerequisite for each perturbation experiment described below. The steady state for the entire model system is defined by the overall carbon and alkalinity balances between inputs from rivers, volcanoes and weathering of organic carbon; and losses to sediment burial and CO_2 consumption during weathering. Additional terms in the steady-state equation account for the alkalinity sink and CO_2 source associated with deep-sea hydrothermal processes. A test of the model's self-consistency is its representation of sedimentation and dissolution in a way that yields a reasonable value for the steady-state global calcite burial flux (*ca.* 1.75×10^{13} mol a^{-1}) (Holland 1978; Mottl 1983) and reasonable values for the steady-state distribution of sediment calcite contents. These conditions were met for each model experiment in this study. To complete the steady-state solution for each experiment, residual terms were introduced to satisfy the steady-state equations for alkalinity and dissolved inorganic carbon in each ocean box. These terms, which were held constant throughout each experiment, represent the processes (such as organic carbon cycling) not treated explicitly by the model. Steady-state concentrations were calculated by iteration of the model using the known history of fossil-fuel CO_2 production to yield model concentrations for the year 1973 that agrees with the volume weighted GEOSECS values (Takahashi *et al.* 1981) and the seasonally-adjusted atmospheric CO_2 measurement from Mauna Loa (Keeling & Bacastow 1977).

The model experiments

Five model experiments were done for this study. Each experiment was a time-dependent simulation of 50000 years. Initial conditions were determined from steady-state solutions to the equations defining each experiment. In each experiment, a 'spike' of CO_2 was injected into the model atmosphere in the form of a CO_2 production function (Keeling & Bacastow 1977) that assured 70% completion in the injection within 100 simulated years and 99% completion within 200 simulated years. The integrated magnitude of the CO_2 spike amounted to 5000×10^{15} g carbon for three of the experiments and 500×10^{15} g carbon in two experiments. Not coincidentally, there are on the order of 5000×10^{15} g carbon in the world's total recoverable fossil fuels (Sundquist 1985; Rotty & Masters 1986). The smaller spike is closer to the cumulative anthropogenic CO_2 production expected in the next few decades (estimated through the year 1988 at 200×10^{15} g carbon from fossil fuels, plus a somewhat smaller contribution from non-fossil sources such as deforestation). The smaller spike is also closer to the magnitude implied by past glacial–interglacial fluctuations.

The five model experiments are summarized in table 1. Experiment 1 was a 'control' experiment in which the model's sediment interactions were deactivated so that calcite dissolution did not respond to the CO_2 spike. Experiment 2 was similar to a previously published fossil-fuel CO_2 simulation (Sundquist 1990), in which calcite dissolution responded in a manner consistent with the relatively high rate constant of 7 d^{-1}, determined experimentally for suspended coccoliths (Keir 1980). Experiment 3 was identical to experiment 2 except that the dissolution rate constant was adjusted to the relatively low value of 0.2 d^{-1}, as observed in laboratory sediment-substrate experiments (Keir 1983). Experiment 4 was identical to experiment 3 except that the magnitude of the CO_2 spike was 10 times smaller. Experiment 5 was identical to experiment 4 except experiment 5 used the relatively high dissolution rate constant of 7 d^{-1}.

As expected, the CO_2 spike induced a pulse of ocean-wide calcite undersaturation in all the experiments. This effect is illustrated by the shoaling of the calcite saturation horizon within a few hundred years of the onset of the experiment (figure 2). In all cases except experiments 4 and 5, the calcite saturation horizon shoaled from its steady-state depth of 3200 m to a minimum depth less than 200 m; the smaller CO_2 spike in experiments 4 and caused the saturation horizon to shoal to only about 2600 m. In each experiment, except the control, the perturbation of the saturation horizon was followed by a slow return to near its initial depth at the end of the 50000-year simulation. This return was caused by the compensating effect of enhanced calcite dissolution. As expected, no calcite compensation was observed in experiment 1; instead, the saturation horizon remained near 200 m because the calcite dissolution response was deactivated.

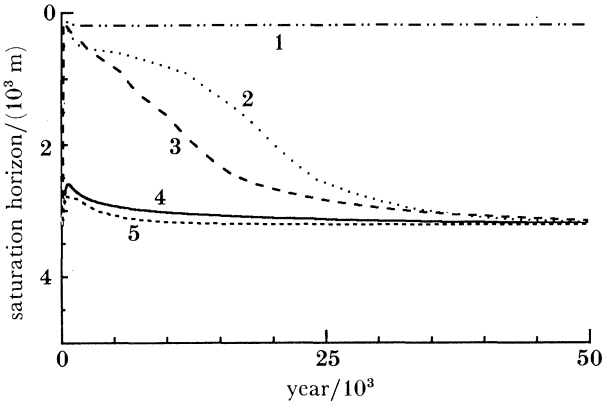

FIGURE 2. Depth of the calcite saturation horizon in the model experiments. The numbered curves correspond to the experiments summarized in table 1.

TABLE 1. SUMMARY OF MODEL EXPERIMENTS

experiment	CO_2 injection 10^{15} g carbon	dissolution?	rate constant
1	5000	no	—
2	5000	yes	high
3	5000	yes	low
4	500	yes	low
5	500	yes	high

The effects of calcite dissolution on the model sediments are exemplified in figure 3, which shows the temporary depletion of calcite in sediments exposed to undersaturated bottom water at depths between 2000 and 3000 m. In experiments 2 and 3, substantial reductions in sediment calcite content were followed by return to near initial conditions by the end of each experiment. This return occurred as the calcite saturation horizon returned to its initial depth and calcite dissolution decreased relative to the particle flux supplying calcite to the sediments. Although the smaller CO_2 spike did cause a calcite dissolution response in experiments 4 and 5, the effect on sediment calcite content was restricted to a much smaller depth range and thus does not appear in figure 3.

Experiments 2 and 3, contrasting the effects of different calcite dissolution rate constants for a large CO_2 perturbation, appear to yield the counter-intuitive result that a lower rate constant (and hence slower dissolution for a given degree of undersaturation) is associated with a more

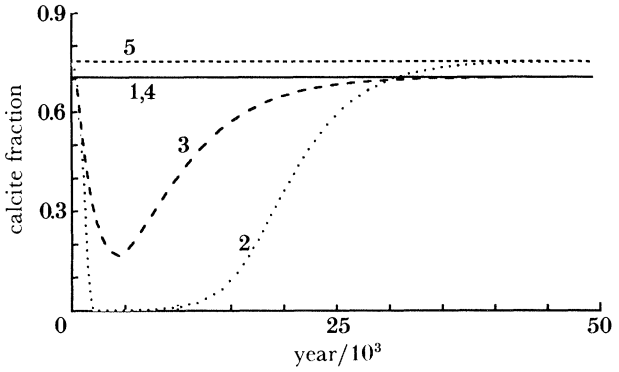

FIGURE 3. Calcite fraction in sediments dissolving at depths between 2000 and 3000 m in the model experiments. The numbered curves correspond to the experiments summarized in table 1.

rapid return to initial conditions after the perturbation. However, these comparisons are obscured by the influence of significant differences between the initial conditions defined by the different steady-state solutions for each experiment. The more rapid calcite dissolution response in experiment 3 probably resulted from the availability of a greater initial steady-state abundance of calcite in sediments deeper than the steady-state saturation horizon. The influence of differing steady states can be minimized in a more rigorous analysis of the response times in these experiments (see below).

Figure 4 shows the atmospheric CO_2 results for all the experiments. The relatively high value that persists to the end of experiment 1 supports the hypothesis that the long-term buffering of atmospheric CO_2 perturbations is significantly reduced in the absence of a calcite dissolution response. The contrast between experiments 4 and 5 suggests that the absolute magnitude of a rapid atmospheric CO_2 perturbation may affect atmospheric CO_2 concentrations for tens of thousands of years. In spite of the differences apparent in figures 2 and 3, experiments 2 and 3 yielded very similar results for atmospheric CO_2. These observations support the suggestion that the long-term response to anthropogenic CO_2 will depend primarily on the magnitude rather than the rate of the perturbation (Sundquist 1990).

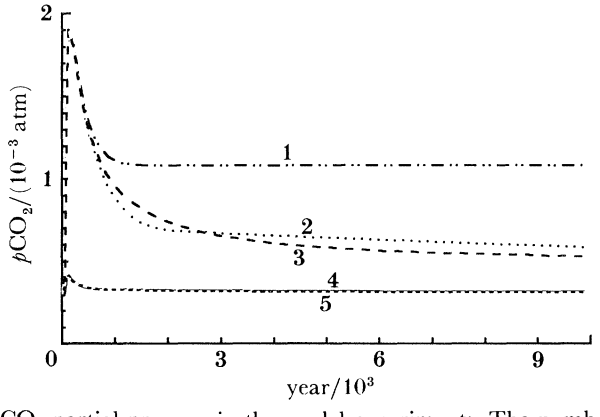

FIGURE 4. Atmospheric CO_2 partial pressure in the model experiments. The numbered curves correspond to the experiments summarized in table 1. The curves for experiments 4 and 5 are nearly identical.

Analysis of response times

Using a model similar in some ways to that used in this study, Keir (1988) suggested that the ocean–sediment response to a global carbon-cycle perturbation can be characterized by two timescales: one corresponding to the mixing time of the oceans, and the other corresponding to a carbonate dissolution response time. Figure 5 shows a similar result for the atmospheric CO_2 results in this study. When these results are plotted on a log scale as differences relative to the value at the end of each experiment, the curves for experiments 2–5 are dominated by two segments. (The steeper slope near the right-hand end of each curve in figures 5 and 6 is an artefact of the fact that the final values at 50000 years are not true steady-state values.) As observed by Keir (1988), the first segment has a relatively steep slope and represents most of the atmospheric CO_2 response, while the second segment is less steep and represents the remainder of the CO_2 response. Keir (1988) attributes 92% of the total response to the first segment. However, comparison of control and dissolution experiments in this study indicates that only 60% of the response can be attributed to the processes actively controlling the first segment in experiments 2 and 3, and only 77% can be attributed to the first segment in experiments 4 and 5. Beyond this segment is a transition to the more gradual slope of the second segment. Experiment 1 demonstrates that the total atmospheric CO_2 buffering without carbonate dissolution is about 60% as effective as the response with carbonate dissolution (see figure 4). The second segment is absent from the curve for experiment 1, supporting Keir's hypothesis that this segment is associated with carbonate dissolution.

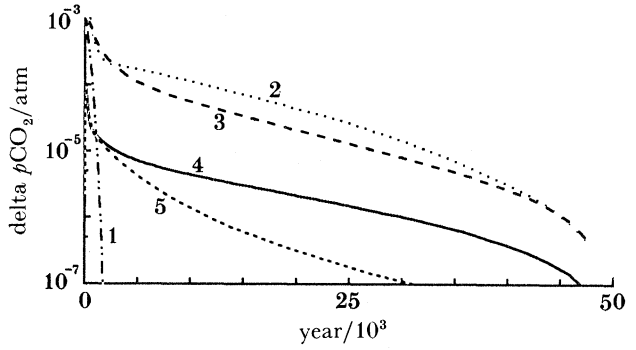

Figure 5. Log-difference against time plots for atmospheric CO_2 in the model experiments. For each experiment, the plotted differences were calculated with respect to the value at 50000 years. The numbered curves correspond to the experiments summarized in table 1.

Table 2 shows 'e-fold' times calculated from the slopes of these segments. The primary (i.e. first segment) response times agree with rates calculated for CO_2 removal from the atmosphere and ocean surface by the ocean mixing parameters used in the model. The processes associated with the primary response are (i) the dissolution of atmospheric CO_2 in the ocean surface; (ii) the 'homogeneous buffering' reactions of dissolving CO_2 with other species in seawater; and (iii) the mixing of ocean surface waters with the remaining volume of the oceans. Because the gas-exchange and homogeneous reactions are relatively rapid, the primary response rate is controlled primarily by the rate of ocean mixing. Results of other model experiments (not shown) confirm the expected sensitivity of the primary response time to variations in the ocean mixing parameters. The rate of the oceanic response to atmospheric CO_2 perturbations appears to be dominated by the rate of vertical ocean mixing.

Table 2. Atmospheric CO_2 response times

experiment	primary response/years	secondary response/years
1	290	—
2	560	10600
3	570	10100
4	280	13800
5	280	6800

However, figure 4 shows clearly that calcite dissolution is very important to the oceans' capacity to buffer atmospheric CO_2. This influence affects the primary CO_2 response times in experiments 2 and 3 (table 2) by substantially lowering the CO_2 values at the end of each experiment, thereby increasing the absolute differences between perturbed CO_2 values and final values. Because of these greater absolute differences, a given CO_2 change is associated with a smaller relative change and a more gradual slope on the log scale of figure 5. Strictly speaking, for a perturbation response to be rigorously attributed to a particular process, analysis of the response should be independent of significant influences by other processes. Accordingly, experiment 1 yields an appropriate primary response time associated with ocean mixing. The similarity among primary response times in experiments 1, 4 and 5 is coincidental; a 'control' experiment identical to experiment 4 except for the absence of carbonate dissolution yielded a CO_2 e-fold response time of 150 years. This result suggests that the effective ocean mixing response time is shorter for smaller atmospheric CO_2 perturbations. It is not clear whether this occurs because the ocean surface buffer factor is lower at the lower atmospheric CO_2 concentrations attained during smaller perturbations or because of some other nonlinear effect in the model.

To examine response times associated with calcite dissolution, the most useful approach is to analyse perturbations in oceanic alkalinity, which is affected in the study by only calcite dissolution. Figure 6 shows volume-weighted average alkalinities plotted on a log scale as differences relative to the value at the end of each experiment. As observed in figure 5, the curves in figure 6 show an initial relatively steep slope followed by a more gradual and persistent slope. The alkalinity curves do not form two segments as distinctly as those for CO_2, and the initial segments account for only about 30–50 % of the total alkalinity response.

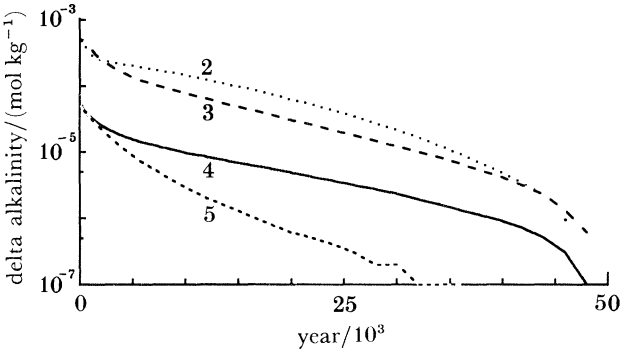

Figure 6. Log-difference against time plots for average ocean alkalinity in the model experiments. Volume-weighted average alkalinities were calculated from the volume and concentration data for the model ocean boxes. For each experiment, the plotted differences were calculated with respect to the value at 50000 years. The numbered curves correspond to the experiments summarized in table 1.

Table 3 shows e-fold times calculated from the slopes of the alkalinity curves in figure 6. Because the only difference between experiments 2 and 3 was the value of the dissolution rate constant, the differing primary (first segment) response times from these experiments suggest that the primary alkalinity response time is controlled by the kinetics of calcite dissolution. This conclusion is supported by the difference between the primary response times of experiments 4 and 5. The primary response time in experiment 4 was nearly identical to that in experiment 3, suggesting that the size of the perturbation does not significantly influence the kinetics of the calcite dissolution response when a relatively low dissolution rate constant is assumed. However, the primary response times of experiments 2 and 5 suggest that, if the dissolution rate constant is assumed to be high, the primary carbonate dissolution response is more rapid for a larger perturbation.

TABLE 3. ALKALINITY RESPONSE TIMES

experiment	primary response/years	secondary response/years
1	—	—
2	1500	11800
3	2600	10800
4	2700	14200
5	2100	6300

The secondary response times in tables 2 and 3 range from about 6000 to 14000 years. The absence of this response in experiment 1 demonstrates that the secondary response is associated with calcite sediment interactions, as suggested by Keir (1988). However, the secondary response time indicated by Keir's model was only 2760 years. Other calculations, based on the 'residence time' of carbonate ions in the ocean, have suggested carbonate compensation response times ranging from 2500 (Broecker & Peng 1987) to 7000 (Broecker 1982) years.

The magnitude of the secondary response times derived in this study, and the consistency of values for both the atmospheric CO_2 and alkalinity secondary response, are consistent with an ocean wide mass-balance origin. Previous studies have suggested that the carbonate-ion response time could be estimated as the quotient of the total abundance of oceanic carbonate ions divided by the global carbonate sedimentation rate, or as the quotient of the carbonate-ion perturbation divided by the corresponding perturbation in the carbonate sedimentation rate. For example, the total carbonate-ion residence time has been estimated recently at 6000 to 7000 years (Broecker 1982; Broecker & Peng 1982). Recent estimates based on perturbation analyses range from 2500 to 6000 years (Broecker 1982; Boyle 1983; Broecker & Peng 1987). The principal uncertainty affecting these calculations appears to be the choice of carbonate sedimentation rates: higher sedimentation rates yield lower residence times.

When comparable calculations are applied to the carbonate-ion abundances and sedimentation rates assumed in the model used in this study, both total-ocean and perturbation analyses yield residence times on the order of 6000–7000 years. It is apparent that some correction factor is needed if the carbonate-ion residence time is indeed related to the longer secondary response time inferred from the model. The necessary correction can be found in an invalid assumption made in nearly all previously published carbonate-ion residence time analyses. Except for the correct analysis of Boyle (1983), previous analyses have assumed that a change in carbonate sediment dissolution or precipitation yields a corresponding mole-for-mole change in the oceanic abundance of dissolved carbonate ions. However, because of

PHILOSOPHICAL TRANSACTIONS OF THE ROYAL SOCIETY A MATHEMATICAL, PHYSICAL & ENGINEERING SCIENCES

reactions involving carbonic and boric acids, the dissolution or precipitation of a mole of calcite changes the carbonate-ion abundance in seawater by only about 0.5–0.6 mol. Accordingly, the estimated range of 6000–7000 years should be corrected to 10000–14000 years for the model used in this study. This range is in excellent agreement with the upper limit of secondary response times compiled in tables 2 and 3. Adjusting the range of previously published carbonate compensation response times (2500–7000 years), the corrected range of estimates becomes 4000–14000 years. However, the conspicuous difference between the secondary response times in experiments 4 and 5 suggests that calcite dissolution kinetics may play a significant role in determining the rate of long-term carbonate compensation response to relatively small perturbations.

Conclusions

As emphasized by Broecker and Peng (1983), Boyle (1983), Keir (1988), and others, the interactions between atmospheric CO_2 and marine carbonate dissolution cannot be characterized by a single timescale. Table 4 summarizes the response times observed in the perturbation experiments described in this study. As suggested by Keir (1988), most of the atmospheric CO_2 response is governed by the rate of vertical ocean mixing. However, calcite dissolution significantly affects the oceans' capacity to buffer changes in atmospheric CO_2. Two response times can be distinguished in the effects of calcite dissolution on ocean–atmosphere chemistry: a relatively rapid response that depends on the kinetics of dissolution in pore waters, and a more gradual response that is controlled by the oceanwide carbonate-ion budget. There is some evidence that the latter can be influenced by calcite dissolution kinetics as well as by the carbonate sedimentation rate.

Table 4. Summary of observed response times

associated process	range of response times/years
homogeneous-buffering–ocean-mixing	150–290
calcite dissolution kinetics	1500–2700
carbonate-ion compensation	6300–14200

These conclusions are subject to many uncertainties. Many important feedbacks and processes have been ignored in the analysis presented here. In particular, the model's treatments of ocean mixing and biology are very crude and do not accommodate the significant circulation and productivity changes that are likely to be associated with the kinds of perturbations that are modelled. The model's representation of sediments is likewise oversimplified, ignoring spatial variations in bioturbation and the potential dissolution response of aragonite and magnesian calcite. The model does not incorporate the possibly important enhancement of carbonate dissolution by the oxidation of organic matter within the sediments (Emerson & Bender 1981; Emerson & Archer, this Symposium). For these reasons, the specific response time suggested here must be viewed as tentative. The principal conclusions of this study are: (i) the relatively rapid buffering of atmospheric CO_2 by seawater is controlled by the rate of ocean mixing and accounts for about 60% of the total buffering by the ocean–sediment system; and (ii) the more gradual buffering of atmospheric CO_2 and seawater by carbonate sediments is controlled by the rate of sedimentation of carbonate particles, but the rate of this buffering is slower than previously thought because the dissolution or precipitation of carbonates does not produce dissolved carbonate ions on a mole-for-mole basis.

References

Arrhenius, G. 1952 Sediment cores from the East Pacific: Swedish Deep-Sea Expedition. (1947–1948) Rep., vol. 5, fasc. I.

Barnola, J. M., Raynaud, D., Korotkevich, Y. S. & Lorius, C. 1987 *Nature, Lond.* **329**, 408–414.

Boyle, E. A. 1983 *J. geophys. Res.* **88**, 7667–7680.

Broecker, W. S. 1982 *Geochim. cosmochim. Acta* **46**, 1689–1705.

Broecker, W. S. & Peng, T.-H. 1982 *Tracers in the sea.* Palisades, New York: Lamont-Doherty Geological Observatory.

Broecker, W. S. & Peng, T.-H. 1987 *Global biogeochem. Cycles* **1**, 15–29.

Broecker, W. S., Peng, T.-H, Mathieu, G., Hesslein, R. & Torgersen, T. 1980 *Radiocarbon* **22**, 676–683.

Culkin, F. 1965 In *Chemical oceanography* (ed. J. P. Riley & G. Skirrow), vol. 1, pp. 121–161. London: Academic Press.

Culberson, C. & Pytkowicz, R. M. 1968 *Limnol. Oceanogr.* **13**, 403–417.

Dickson, A. G. & Riley, J. P. 1979 *Mar. Chem.* **7**, 101–109.

Emerson, S. and Bender, M. 1981 *J. Mar. Res.* **39**, 139–163.

Gordon, A. L. & Taylor, H. W. 1975 In *Proc. symp. numerical models of ocean circulation*, pp. 54–59. Washington, D.C.: National Academy of Sciences.

Gorshkov, S. G. 1980 *Ocean atlas reference tables* (in Russian), Department of Navigational Oceanography, Ministry of Defense, U.S.S.R. (156 pages).

Holland, H. D. 1978 *The chemistry of the atmosphere and oceans.* New York: J. Wiley.

Ingle, S. E. 1975 *Mar. Chem.* **3**, 301–319.

Keeling, C. D. & Bacastow, R. B. 1977 In *Energy and climate*, pp. 72–95. Washington, D.C.: National Academy of Sciences.

Keir, R. S. 1980 *Geochim. cosmochim. Acta* **44**, 241–252.

Keir, R. S. 1983 *Deep Sea Res.* **30**, 279–296.

Keir, R. S. 1988 *Paleoceanography* **3**, 413–445.

Ku, T. L., Huh, C. A. & Chen, P. S. 1980 *Earth planet. Sci. Lett.* **49**, 293–308.

Li, Y.-H, Peng, T.-H., Broecker, W. S. & Ostlund, H. G. 1984 *Tellus* B **36**, 212–217.

Lyman, J. 1957 Buffer mechanism of seawater, Ph.D. thesis, University of California, Los Angeles, U.S.A.

Mehrbach, C., Culberson, C. H., Hawley, J. E. & Pytkowicz, R. M. 1973 *Limnol. Oceanogr.* **18**, 897–907.

Menard, H. W. & Smith, S. M. 1966 *J. geophys. Res.* **71**, 4305–4325.

Millero, F. J. 1979 *Geochim. cosmochim. Acta* **43**, 1651–1661.

Mottl, M. J. 1983 *Bull. geol. Soc. Am.* **94**, 161–180.

Rotty, R. M. & Masters, C. D. 1986 In *Atmospheric carbon dioxide and the global carbon cycle* (ed. J. R. Trabalka), pp. 63–80. Washington, D.C.: U.S. Department of Energy.

Seigenthaler, U. 1983 *J. geophys. Res.* **88**, 3599–3608.

Sundquist, E. T. 1985 In *The carbon cycle and atmospheric* CO_2*: natural variations archean to present* (ed. E. T. Sundquist & W. S. Broecker), pp. 397–411. Washington, D.C.: American Geophysical Union.

Sundquist, E. T. 1990 In *Sea level change.* Washington, D.C.: National Academy of Sciences.

Sundquist, E. T., Richardson, D. K., Broecker, W. S. & Peng, T.-H. 1977 In *The fate of fossil fuel* CO_2 *in the oceans* (ed. N. R. Andersen & A. Malahoff), pp. 429–541. New York: Plenum.

Takahashi, T., Broecker, W. S. & Bainbridge, A. E. 1981 In *Carbon cycle-modelling, SCOPE* **16**, (ed. B. Bolin), pp. 271–286. New York: J. Wiley.

Weiss, R. F. 1974 *Mar. Chem.* **2**, 203–215.

PHILOSOPHICAL TRANSACTIONS OF THE ROYAL SOCIETY A MATHEMATICAL, PHYSICAL & ENGINEERING SCIENCES